REPORT R-656 JULY, 1974 UILU-ENG 74-2222

CSL COORDINATED SCIENCE LABORATORY

DIRECT IDENTIFICATION OF ATOMIC BINDING SITES ON A CRYSTAL

WILLIAM R. GRAHAM
GERT EHRLICH

UNIVERSITY OF ILLINOIS - URBANA, ILLINOIS

DIRECT IDENTIFICATION OF ATOMIC BINDING SITES ON A CRYSTAL

by

WILLIAM R. GRAHAM AND GERT EHRLICH

This work was supported by the Air Force Office of Scientific Research (AFSC), USAF, under Grant AFOSR 72-2210, and operated under the Joint Services Electronics Program (U.S. Army, U.S. Navy, and U.S. Air Force) under Contract DAAB-07-72-C-0259.

DIRECT IDENTIFICATION OF ATOMIC BINDING SITES ON A CRYSTAL*

By William R. Graham and Gert Ehrlich
Coordinated Science Laboratory† and Department of Metallurgy
University of Illinois at Urbana-Champaign
Urbana, Illinois 61801

ABSTRACT

The atomic resolution of the field ion microscope, in conjunction with its ability to remove and identify individual atomic layers, has been used to map unambiguously the unit cell of the (111) plane of tungsten and to determine directly the location of single tungsten atoms adsorbed on this plane. Adatoms have been observed to occupy two binding sites only. The predominant site corresponds to a normal lattice position. The second site is of similar symmetry, in that the adatom sits between three first layer atoms; however, at this position the adatom is located above an atom in the second rather than the third lattice layer. The former site is favored energetically, but only by $\approx \frac{1}{2}$ eV. All observations have been made at high fields, but it is shown from studies of migration and other effects that the binding sites identified in the field ion microscope are typical of a normal, field free environment.

---

* Supported by the Air Force Office of Scientific Research (AFSC), USAF, under Grant AFOSR 72-2210.

† Operated under the Joint Services Electronics Program (U.S. Army, U.S. Navy, and U.S. Air Force) under Contract DAAB-07-72-C-0259.

1. INTRODUCTION

Vital to an understanding of the surface behavior of solids is a knowledge of the structure and atomic arrangement at the interface. Such information is still quite fragmentary. One fundamental question which has not yet been resolved is--where on a crystal are single adsorbed atoms held? It is to an experimental solution of this problem that we will address ourselves.

For adsorbed monolayers much has already been done to study the atomic arrangement using low energy electron diffraction (LEED). A sketch of the present understanding of such layers, and of LEED,[1] is therefore necessary as an introduction to our own studies, which are focussed on the location of single atoms.

The first step in defining the location of atoms in an overlayer with respect to those of the underlying crystal was taken by Park.[2,3] He showed that the splitting of the fractional order spots in c(2x2) patterns, typical of adsorption on (100) planes, was due to scattering from antiphase domains in which atoms were held at sites of four-fold symmetry. This limits the type of binding site for atoms in the adsorbed layer without, however, defining it unequivocally. Only recently has there been substantial progress in this direction, based on a detailed examination of scattering intensity. Two different approaches are being pursued in dealing with the complicated dynamical effects which obscure the intensity relations in low energy

electron diffraction from monolayers:

1. Averaging of the experimental diffraction intensities, to strip away dynamical contributions.

2. Comparison of scattering intensities with the results of fully dynamical calculations for different monolayer arrangements.

The first of these methods,[1a] which is quite promising for clean surfaces, has been explored for only one overlayer: the c(2x8) coincidence lattice formed at high temperatures by oxygen on the (100) plane of rhodium.[4] There have been several attempts of the second type. From a comparison of the experimental intensities with those calculated for sodium on the (100) plane of nickel, Andersson and Pendry[5] concluded that the alkali atom was positioned above a hole of four-fold symmetry in the (100). Forstmann et al.,[6] using similar procedures, analyzed iodine layers on the (111) of silver. Best agreement with the experimental measurements was obtained for iodine in hollows of three-fold symmetry. Two such sites are possible on the (111): one with, and the other without a lattice atom in the 2nd lattice layer directly below the hollow. Sites of the latter type emerged as the most likely position for atoms in the iodine film.

Most recently, three different groups[7-9] have concentrated on the arrangement of chalcogenide layers on the (100) plane of nickel. These analyses, based on comparable experiments, arrive at the same overall geometry: the atoms in the overlayer are viewed as sitting in four-fold symmetric hollows. However, the distances between the

overlayer and the surface deduced by the three groups differ considerably. Despite a stated uncertainty of only $\pm$ 0.1 Å for oxygen on nickel, values of 0.90,[7] 1.5,[8] and 1.8 Å[9] have been reported. Although all these studies on overlayers agree in placing the adatoms in recessed positions, at which they enjoy high coordination with the surface, it appears from the results so far that further work is desirable to make structural information obtained by diffraction methods truly reliable.

In overlayers, we are dealing with adatoms interacting not only with the lattice, but with each other as well. The more elementary task of defining the sites at which single adatoms are held on a crystal has not been touched. Our approach to this problem is straightforward--it depends on our ability to depict single atoms, both in the surface layer and on top of it, using the field ion microscope. We can expect to establish the position of an adatom projected onto the plane of the substrate on which it is held. From field ion microscopy[10] the spacing of atoms perpendicular to the substrate is not accessible; neither is absolute information on spacings at the surface. In this regard the technique is inferior to diffraction methods. However, field ion microscopy is particularly suited for the study of single atoms, an area in which low energy electron diffraction has not as yet been successfully employed.

In what follows we outline the first attempt to establish the location of adatoms on a crystal surface by direct observation. For this introductory effort we have selected tungsten, the material most

intensively studied in the field ion microscope. One precondition for success in such a venture is the ability to define the location of every atom in the surface itself. For the low index planes of the body-centered cubic lattice, this criterion is best met by the (111) plane, and it is on this surface that we have concentrated. To minimize possible difficulties, we have made all our observations on tungsten adatoms self-adsorbed on their own lattice; it will be obvious, however, that the procedures developed here are equally applicable to a wide range of planes and adsorbed entities.

2. EXPERIMENTAL TECHNIQUES

A simple but versatile field ion microscope has been used in this study. The tube shown in Fig. 1 is equipped with an internal image intensifier, based on a 1 in. diameter channel plate.[11] Centering of the image on the screen is possible by adjusting bellows, which join the sample holder to the imaging section of the microscope. The two are connected by a 4 in. flange to facilitate rapid disassembly of the microscope. The specimen under examination is spot-welded onto a .007 in. diameter tungsten loop, 2 in. long, which in turn is mounted on two pins of a four lead press at the bottom of a small coldfinger. The other two pins support potential leads, for direct measurement of the loop temperature during resistive heating. Specimen temperatures down to 5^{o} K can be achieved by manual control of the flow of liquid helium to the bottom of the coldfinger. Temperatures at the coldfinger are

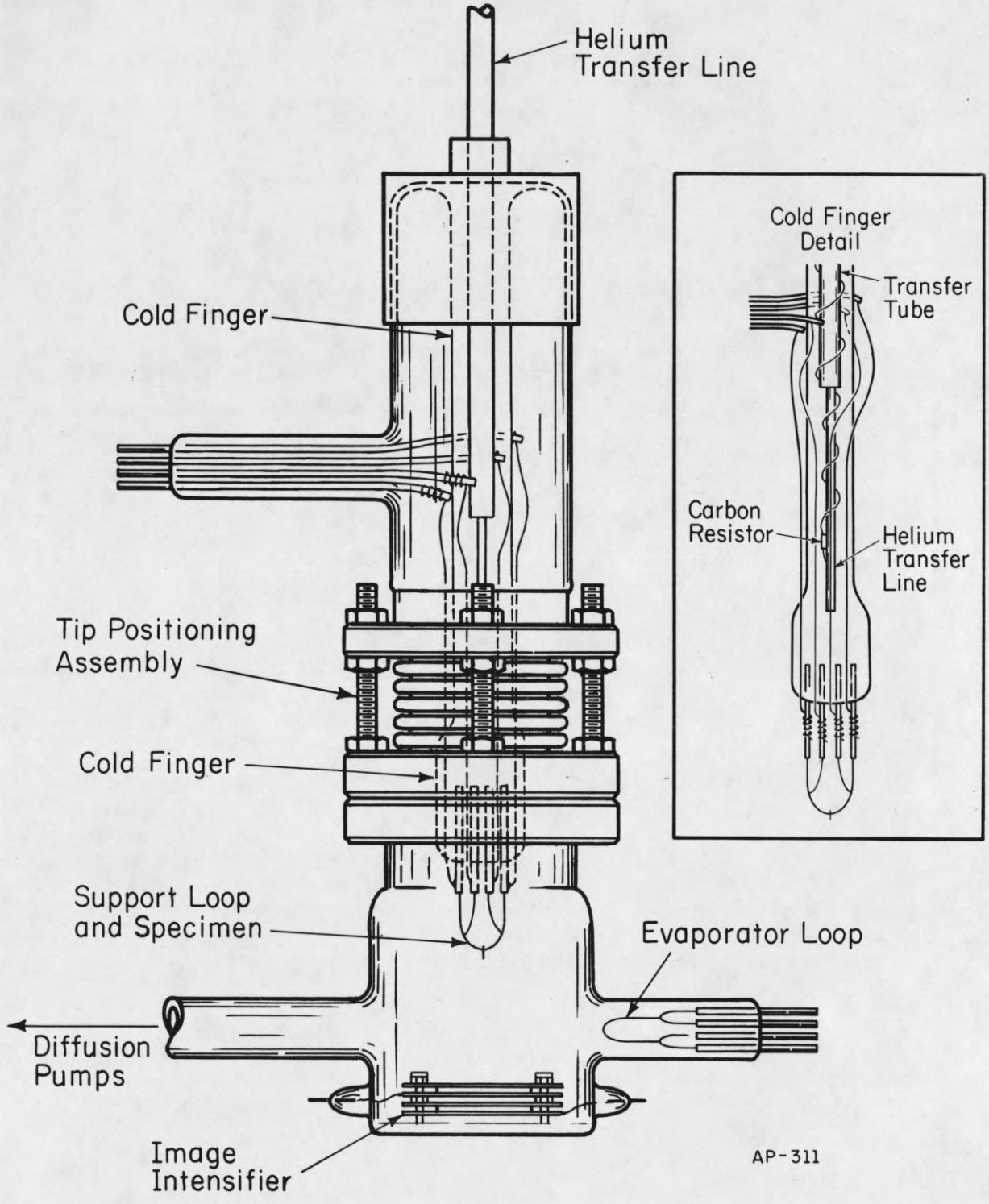

Fig. 1. Field ion microscope with channel plate image intensifier and adjustable tip positioner.

monitored by measuring the resistance of a 1000 Ω carbon resistor (Allen-Bradley), mounted at the end of the stainless steel transfer tube through which liquid helium is introduced. Specimens are made from .005 in. diameter tungsten wire oriented along the [111], obtained from the Field Emission and Ion Sources Corp., McMinnville, Oregon, and are sharpened by electropolishing in 2N NaOH using an automatic drop-off method.[12]

Either the tip or the imaging section of the microscope can be operated at high voltage, making it possible to heat the specimen during imaging. Resistive heating of a .007 in. diameter tungsten loop, mounted in a side arm in line of sight with the specimen, provides atoms for deposition onto the surface. The microscope is part of a small ultrahigh vacuum station, largely built of glass, and evacuated by mercury diffusion pumps with a speed of $\approx$ 40 liters/sec. Two imaging gases are available. Neon, stored in a 1 liter bulb, can be admitted to the gas handling system through a Granville-Phillips Type C valve; helium can be introduced through a Vycor diffuser.

Ultrahigh vacuum conditions are achieved in the microscope by the usual repeated cycle of baking followed by outgassing of the metal parts. To avoid degrading the channel plate, the system temperature is never raised above 320° C. The channel plate is itself a particularly plentiful scource of contamination; when first installed in the system, it is outgassed for many days by bombardment with field emitted electrons drawn from the sample. A new specimen is similarly

subjected to a rigorous treatment, which includes heating to 1000° K for approximately 24 hours and repetitive flashing to higher temperatures for periods of a few seconds. After outgassing of the vapor source, by resistive heating to just below the temperature at which atoms are deposited on the sample, the specimen is field evaporated to produce the atomically smooth endform. For this, as well as imaging, a highly stabilized dc power supply is used with regulation of $\pm$ .001%. Pulse desorption is carried out, when necessary, with a unit delivering 2 μsec pulses at voltages adjustable from 0 to 15 kV.

The rate of contamination of the field evaporated surface, as measured by changes in the field emission of electrons, serves as a direct indicator of the cleanliness. Measurements are carried out only if the voltage to maintain a field emission current of 5×10^{-9} A varies by less than 0.5%/hr. The cleanliness of the vapor source is checked in two ways. After heating to just below the evaporation temperature, the emitting surface has to remain clean as judged by field emission. Experiments are continued only if during actual evaporation the pressure rise in the system amounts to less than 2×10^{-11} mm.

The location of adatoms deposited in this way on the surface has been recorded photographically, using a Canon FL camera with an inverted f/1.2 lens of 58 mm focal length, mounted rigidly to the tabletop holding the microscope. All micrographs were taken on Kodak Tri-X, at $\approx$ 5 seconds exposure, with the lens stopped down to f/2.8. Image gas pressures are typically 2×10^{-5} mm. In routine operation the channel plate is set at 1200 V with the accelerating voltage between plate and fluorescent screen at 4.2 kV.

3. ATOMIC ARRANGEMENT OF THE (111) PLANE

To define where on a surface individual adatoms are held, it is first necessary to establish the location of the atoms which make up the surface. With the (111) this is not a trivial task, and this section is therefore devoted entirely to this problem.

For (111) planes with a diameter less than 25 Å, every atom in the surface layer is clearly resolved, as in the micrograph of a (111) oriented tungsten surface in Fig. 2. It should be noted parenthetically that such images are best obtained at a voltage $\approx$ 4% below that most suitable for imaging the tip as a whole. The relation of the (111) to the overall atomic arrangement of the emitter, as well as to other planes, is clarified by the model in Fig. 3. In the field ion micrograph we at best see the outermost atoms shown in the model, the edges and corners of planes; on a few selected surfaces, such as the (111) and (411), every atom in the first lattice layer appears clearly. This, however, is not enough. The arrangement of atoms[13] forming a (111) plane in the body-centered cubic lattice is indicated schematically in Fig. 4. It is immediately apparent that the atoms in the first lattice plane do not alone define the structure of the surface. However, from the model in Fig. 3 it is evident that the unit parallelogram is always pointed away from the (211) planes on the tip. An idea of the orientation of the unit cell can therefore be obtained from the ion micrograph of the tip as a whole, in Fig. 2. However, for an unequivocal definition

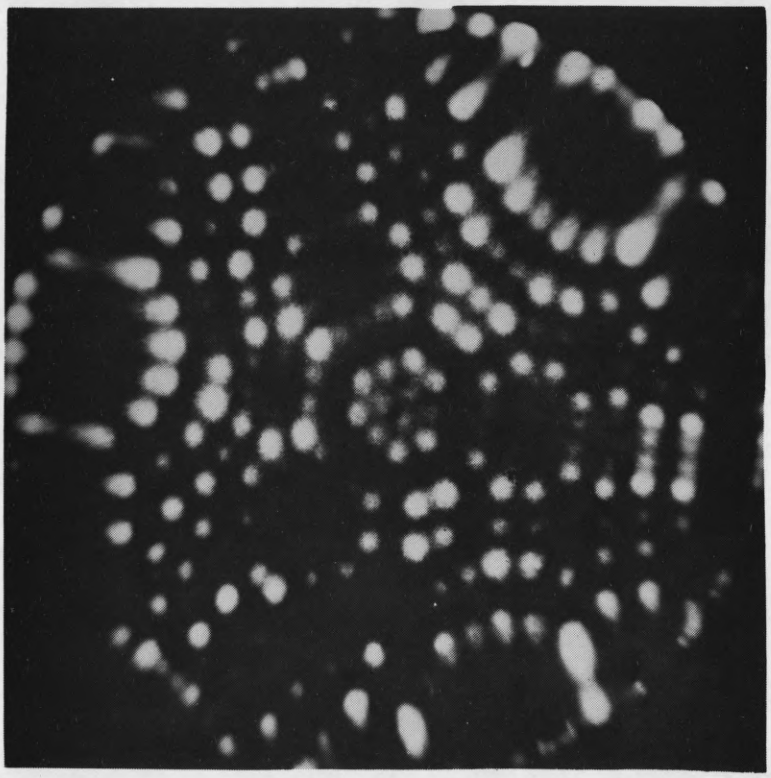

Fig. 2. Field ion micrograph of [111] oriented tungsten emitter, obtained by field evaporation in He at 20° K. (111) plane has been tailored by pulsed field evaporation to reveal every atom.

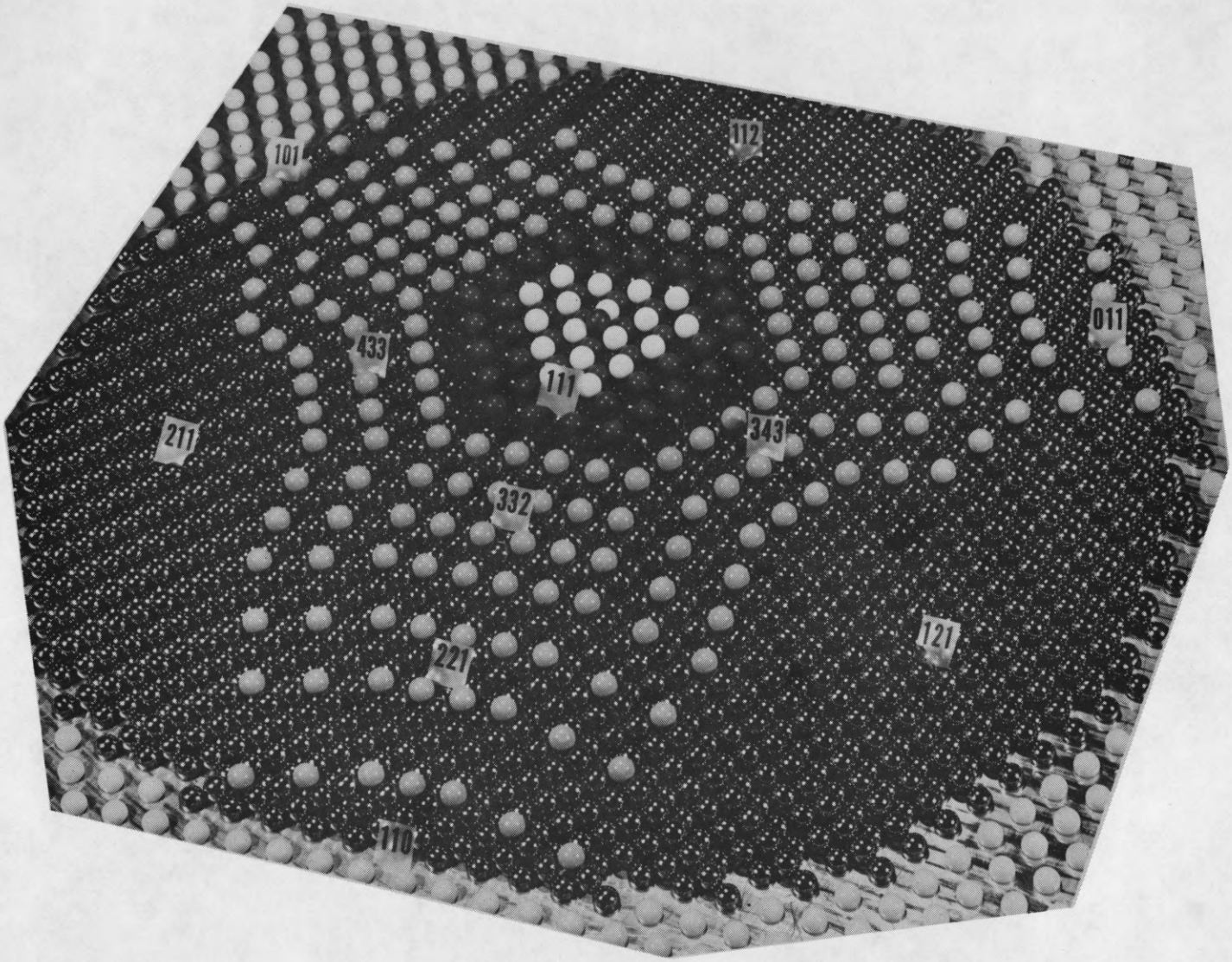

Fig. 3. Hard-sphere model of bcc emitter oriented along [111]. Size is scaled to that of specimens in the present experiments.

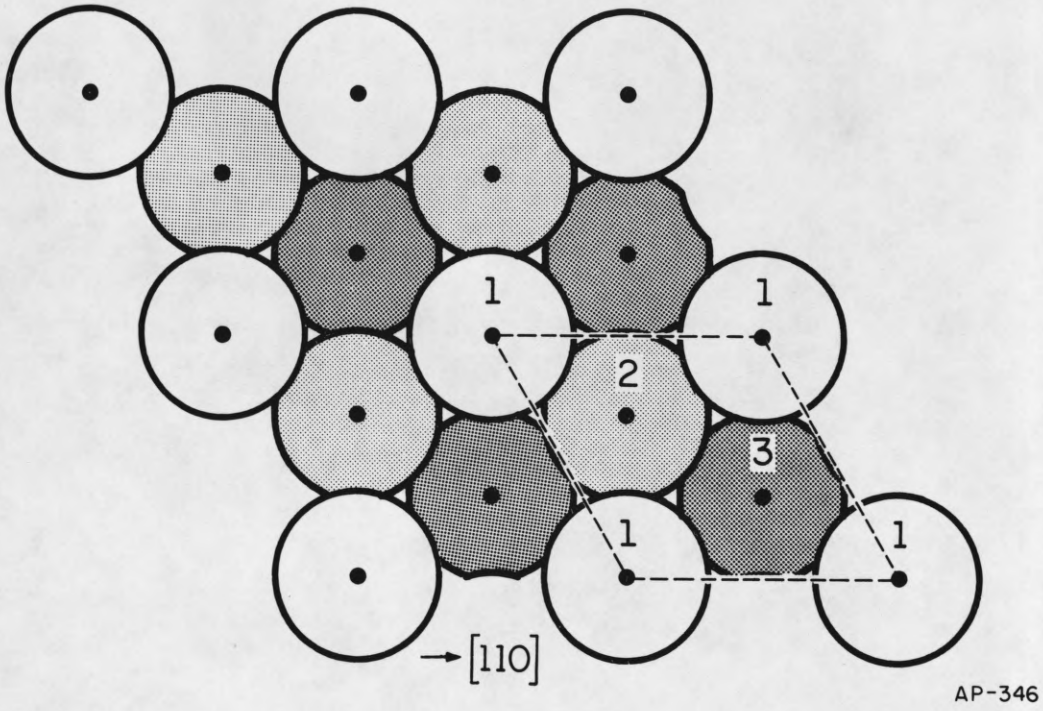

Fig. 4. Map of atomic arrangement of (111) plane of tungsten. a = lattice spacing. Numerals and shading indicate vertical position of atom layer: Layer 1 = surface; 2 = $-a(2\sqrt{3})$; 3 = $-a/\sqrt{3}$.

of the structure of the (111), which is a prerequisite to any attempt at identifying the sites at which an adatom may be held, it is best to establish the positions of atoms in the second lattice plane.

The atomic arrangement of the (111) can be defined[14] quite unequivocally by locating the atoms in both the first and second lattice layers. First the position of atoms in the outermost layer is established by field ion microscopy. This layer is then removed by pulsed field evaporation, with the ion image under continuous observation. Pulses 20% above the best image voltage, applied at a rate of 50 per second, make it possible to remove the first layer essentially atom by atom, until the second layer is visible. The image of the second layer superposed on that of the first layer then defines the surface unit cell. That this procedure is reliable can be checked by removing three consecutive layers from the surface. It is clear from the diagram of the unit cell in Fig. 4 that the fourth layer exactly duplicates the first. The image of the (111) after removal of three layers should therefore superpose precisely on that of the starting surface.

An actual field evaporation sequence of four consecutive layers of the (111) plane of tungsten is shown in Fig. 5, and a photographic superposition of the first upon the fourth layer in this sequence is displayed in Fig. 6. That the positions of the atoms in these two layers do indeed coincide can best be appreciated from Fig. 7. In this, the centers of atoms in the fourth layer of the (111) were located by

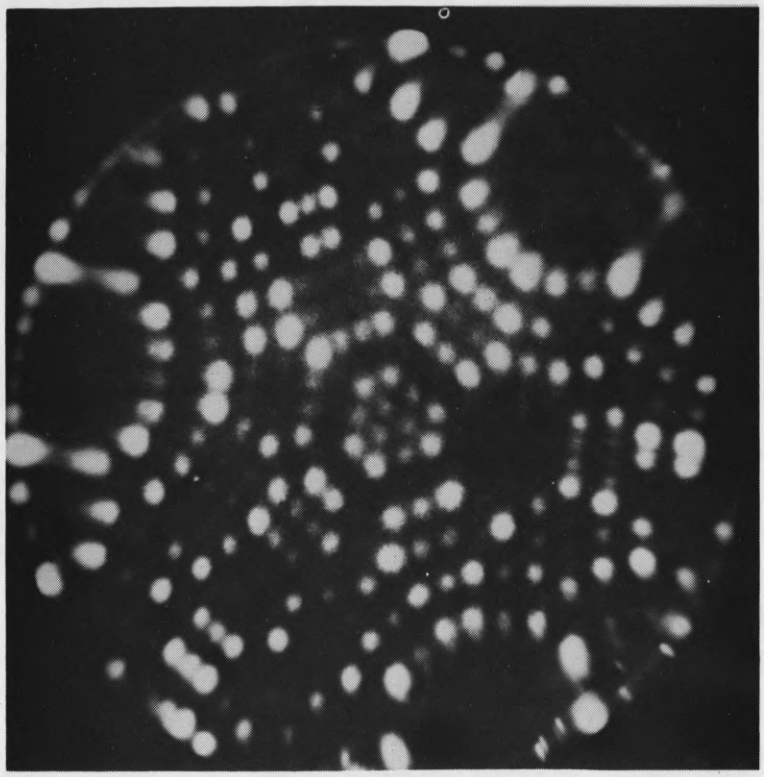

Fig. 5a. Field evaporation sequence of the first through the fourth atom layer of the (111) plane; first layer, after trimming to reveal individual atoms.

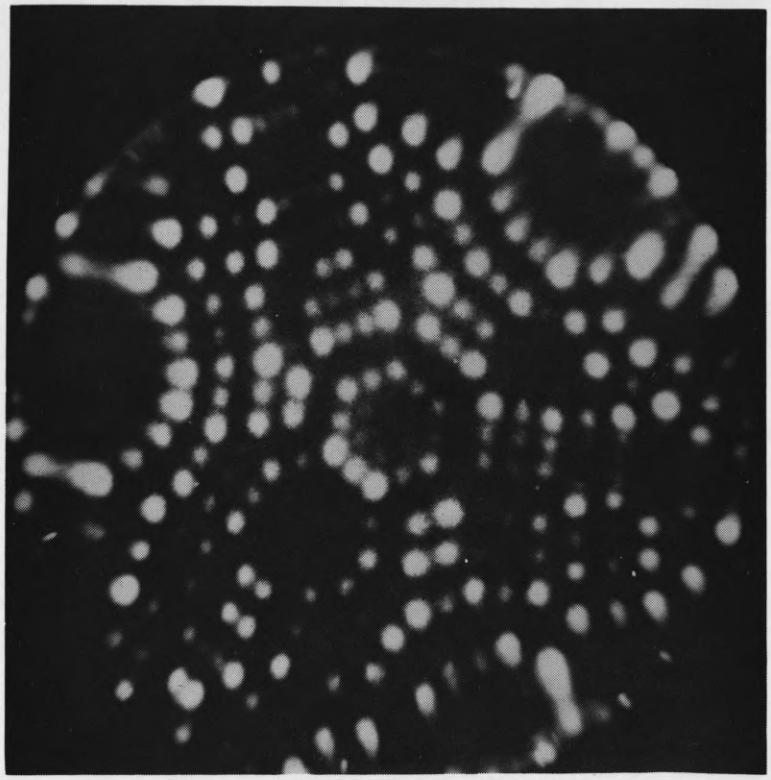

Fig. 5b. Field evaporation sequence of the first through the fourth atom layer of the (111) plane; 2nd layer.

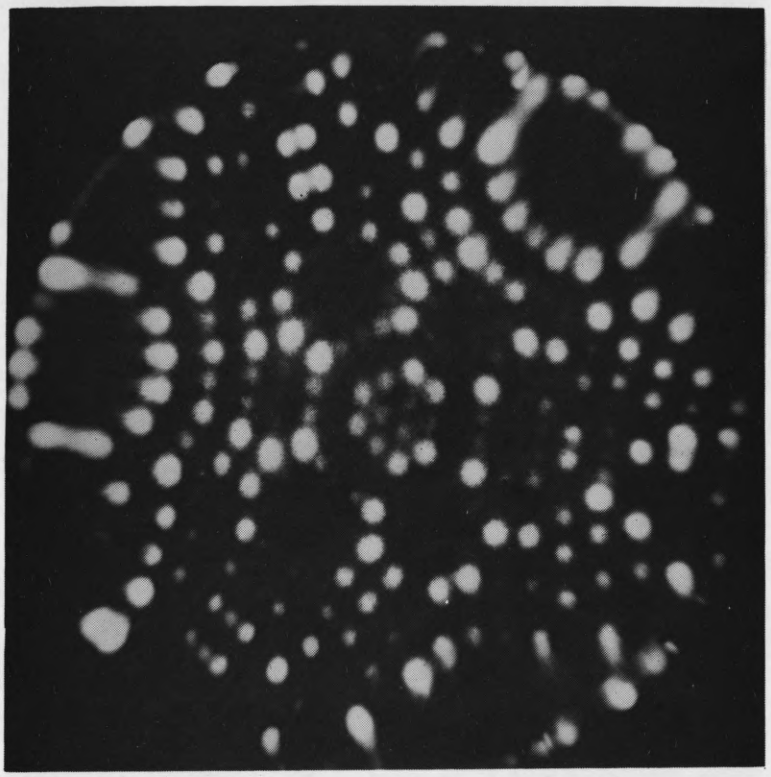

Fig. 5c. Field evaporation sequence of the first through the fourth atom layer of the (111) plane; 3rd layer.

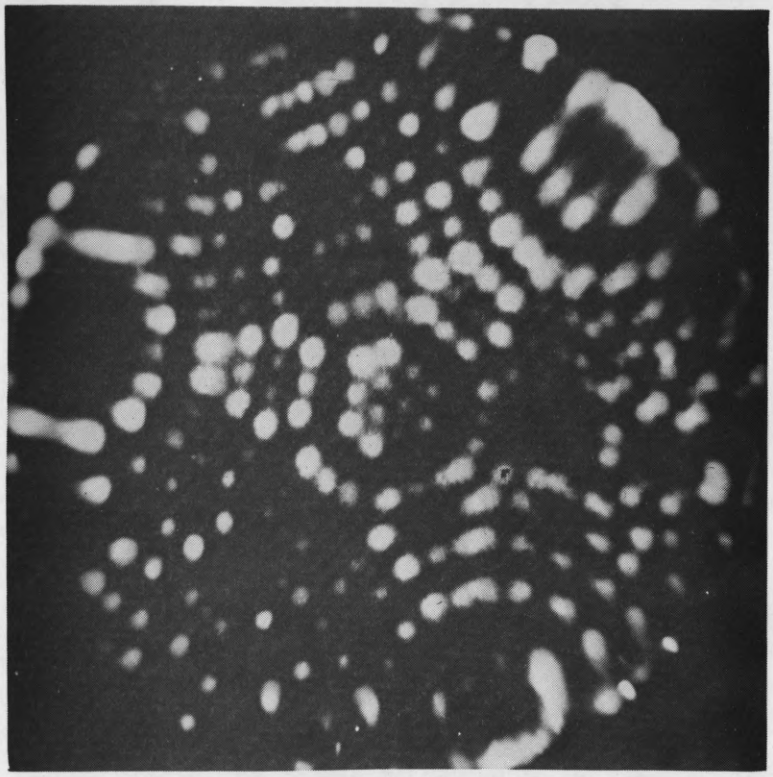

Fig. 5d. Field evaporation sequence of the first through the fourth atom layer of the (111) plane; 4th layer

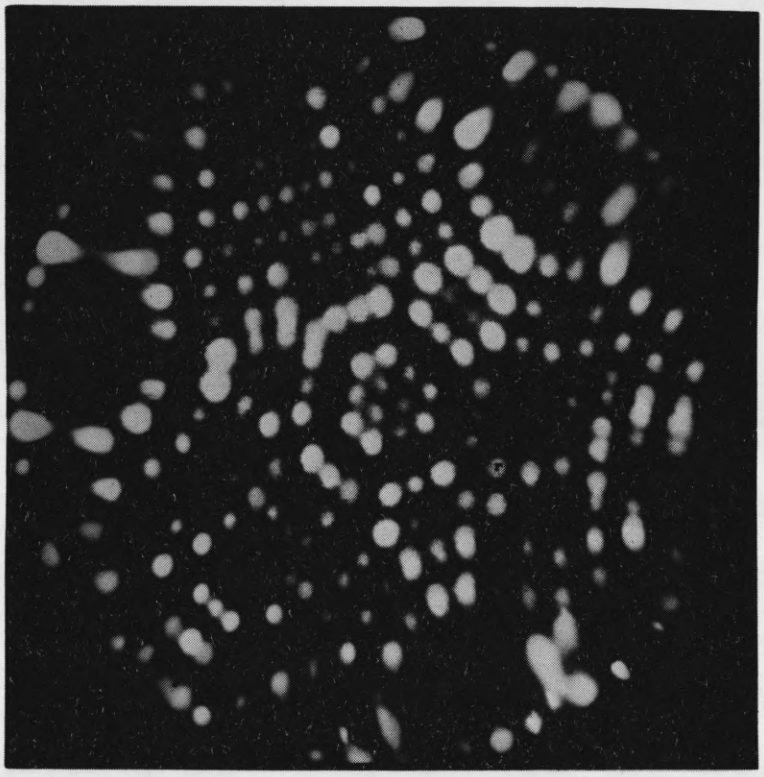

Fig. 6. Superposition of 1st layer of the (111) plane upon 4th; that is, of Fig. 5a upon 5d. Location of atoms is identical, as expected.

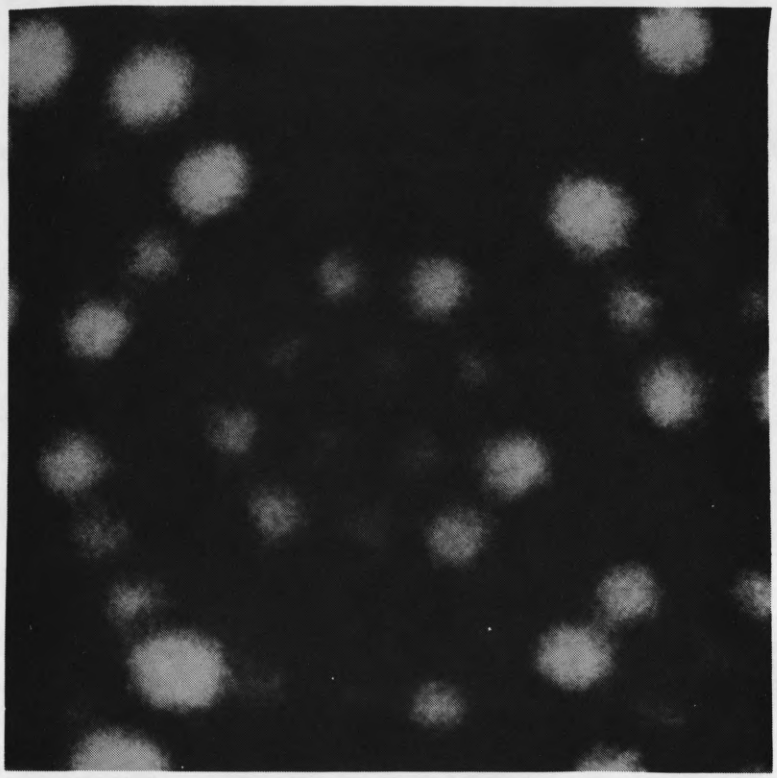

Fig. 7a. Detailed view of (111) plane; 1st atom layer.

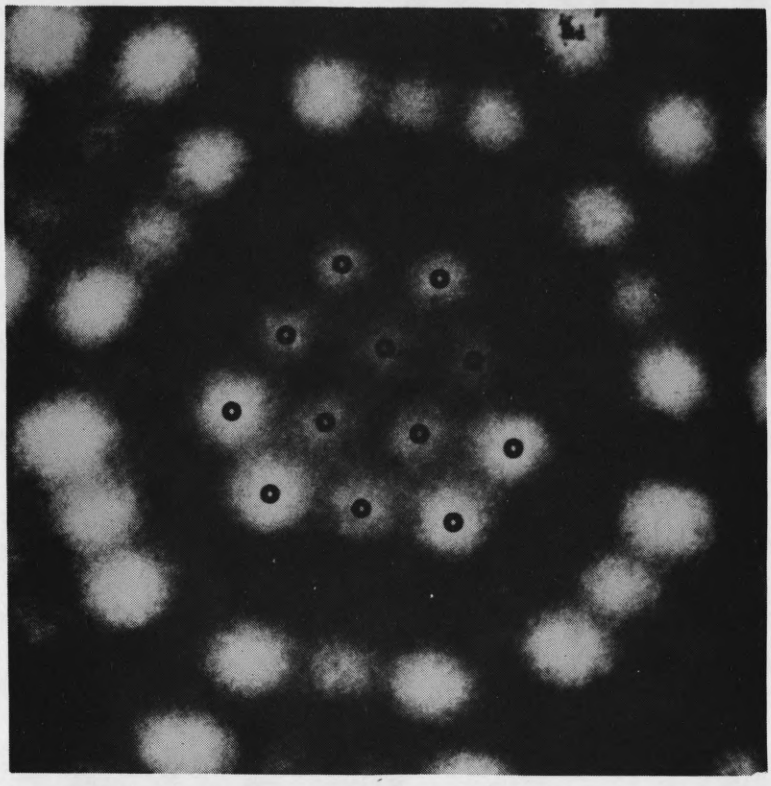

Fig. 7b. Detailed view of (111) plane; 4th layer, with atom centers marked.

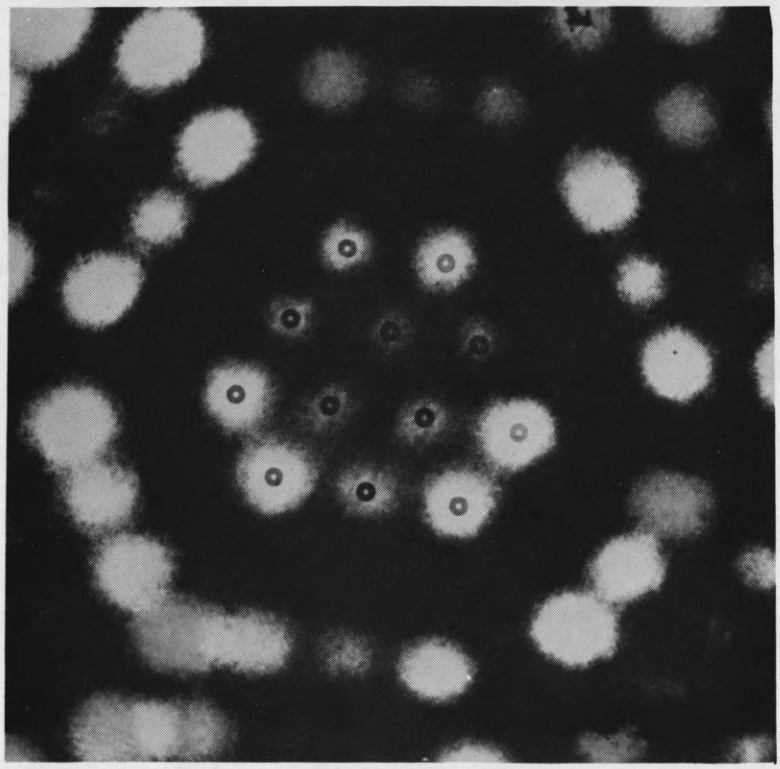

Fig. 7c. Detailed view of (111) plane; superposition of (b) on (a).

dots; a photograph of the surface so marked (Fig. 7b) was then superposed on the image of the fourth layer by relying on fiducial marks on both, to give Fig. 7c. The locating marks for layer 4 are seen to coincide with the centers of the atoms in layer 1 to within $\pm$ 0.3 Å. The error is largely due to the difficulty of imaging consecutive planes at identical intensities for each atom. There is no persistent error in locating atoms. This can easily be established by just continuing field evaporation. The superposition of the fourth on the tenth layer, in Fig. 8, is just as good as that on the first, in Fig. 6.

This technique of identifying the unit cell of the (111) has been proven in more than 100 trials on [111] oriented tungsten. It must be emphasized, however, that for samples prepared from [110] oriented wire, this method is not reliable: atoms in the 4th layer commonly do not meet the superposition criteria. The reason for this has not been examined in depth. However, on several occasions an apparent sideways slip of several atoms in the first layer has been observed on the (111). Such slip is presumably facilitated by non-radial forces generated at the off-axis (111) when high voltages are applied. Whatever the cause of these difficulties, they do not intrude in [111] oriented specimens. For these, we have in hand a reliable method for establishing the atomic arrangement of the (111) plane.

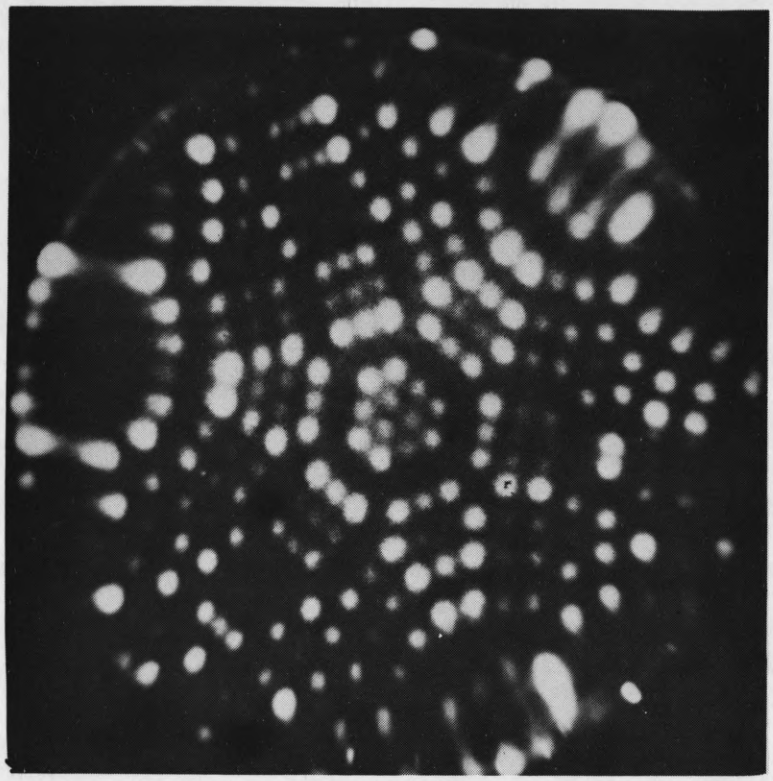

Fig. 8. Continuation of field evaporation sequence: superposition of the 10th layer upon the 4th, previously shown in Fig. 5d.

4. LOCATION OF INDIVIDUAL ADATOMS

4.1 Procedures

With the field ion microscope we cannot hope to determine all the interatomic distances necessary to define the location of an adatom with respect to the atoms of the underlying lattice. Vertical separations cannot be measured at all, and an absolute assessment of distances in the plane of the surface is also difficult. However, it should be possible to distinguish between a few locations on the (111), selected for their high symmetry, as conceivable sites for binding of adatoms. These possible sites are apparent from the diagram of the (111) plane in Fig. 4. An adatom could conceivably be held right on top of a lattice atom, or on the ridge between two atoms in the first layer. Intuitively these are not very likely, as there exist sites at which the adatom enjoys higher coordination with the lattice. On the (111) there are two such possibilities, both of trigonal symmetry: one above atom 2, the other above atom 3 in the unit cell. At the former an adatom is surrounded by three first layer atoms and by an atom in the second lattice layer. At site 3 the adatom is again surrounded by three first layer atoms, but is now directly over an atom in the third lattice layer. This, in fact, is the site occupied in forming a new lattice layer; as such we will refer to it as a lattice site. A layer started by placing an adatom above atom 2 constitutes a stacking fault; this position will therefore be designated as a fault site.

We have already demonstrated, in the last section, our ability to define the unit cell of the (111) plane, that is, to locate and distinguish the sites just enumerated. To now establish the binding sites for adatoms, it is in principle necessary only to find out where on the (111) an atom deposited from the vapor is actually located. In practice there are still problems to overcome.

When an atom is deposited on a small, totally resolved (111), such as the plane shown in Fig. 2, the image of the adatom is much larger than that of the lattice atoms. This is a well-known effect.[15] At a highly protruding atom the rate of ionization is enhanced, increasing the image intensity and therefore also the size of the recorded image spot. This effect is especially significant for small planes. In fact, the spot size of the adatom is so large that it is not possible to define with any accuracy the location of the adatom relative to the atoms of the substrate. On large (111) planes, sharp, well defined images of an adatom can be achieved; however, on such a surface the atoms of the substrate cannot be resolved, because of the diminution in the electric field towards the center. To surmount this difficulty we have devised the following procedure.

An adatom is deposited on a relatively large (111) plane (diameter > 30 Å) and its position is recorded photographically, as in Fig. 9a. The adatom is then removed by pulsed field evaporation at $\approx 15^{\circ}$ K (Fig. 9b). Field evaporation of the underlying (111) is carefully continued, until a sufficient number of atoms has been removed

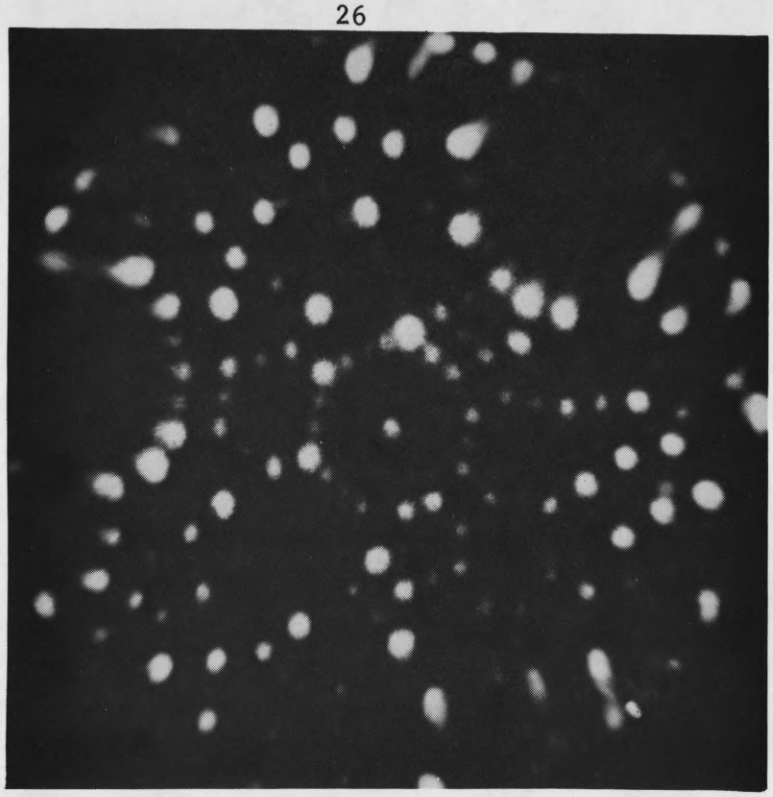

(a)

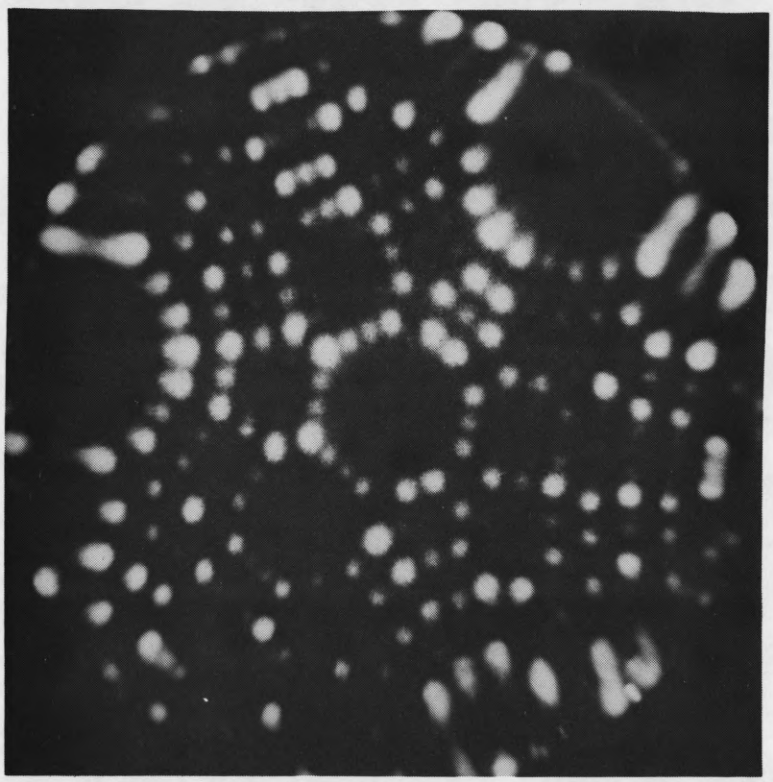

(b)

Fig. 9. Steps in locating position of adatom on (111) plane.
a. W atom, deposited on a large (111) plane by evaporation from incandescent filament.
b. Adatom removed by field desorption at $\approx 15^{\circ}$ K.

from the edge for all the remaining atoms of the (111) to be clearly resolved. At this stage another photograph is taken, shown in Fig. 9c. Finally, the previously recorded image of the adatom, in Fig. 9a, is superposed upon the photograph of the fully resolved (111) of Fig. 9c, to yield the composite in Fig. 9d. From this superposition it is possible to obtain a clearly defined view of the location of the adatom relative to the atoms of the first lattice layer. In order to verify the validity of this identification procedure, and to confirm the unit cell of the (111), the outermost layer of the (111) plane and two further layers are then stripped by field evaporation. The fourth layer of the (111) so exposed is imaged and recorded. The image of this layer must, of course, superpose upon that of the original (111) to validate the sequence.

Such a sequence of observation must meet several stringent requirements to be considered significant:

1. When first deposited on the (111), the adatom has to fall close to the center of the plane, in a region encompassing at most 12 to 14 atoms of the first lattice layer. This is necessary to minimize the distortion of the field ion image inevitable for adatoms close to the edges of the small planes which can be imaged with every atom resolved.

2. Fiducial marks in the channel plate have to be clearly visible in all the photographs of a sequence, from the image of an adatom on a large plane down to the shot of the fully resolved fourth lattice layer.

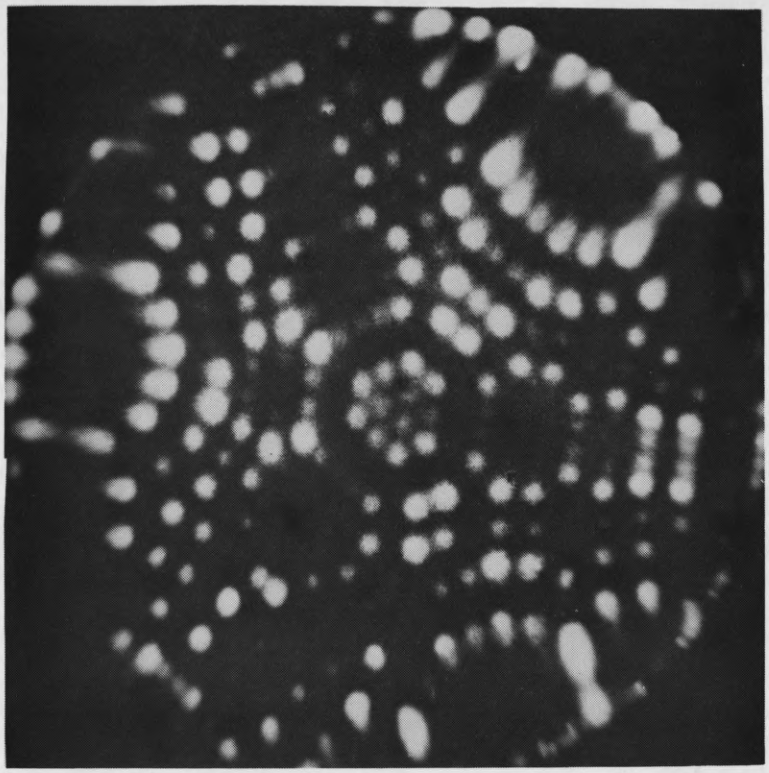

(c)

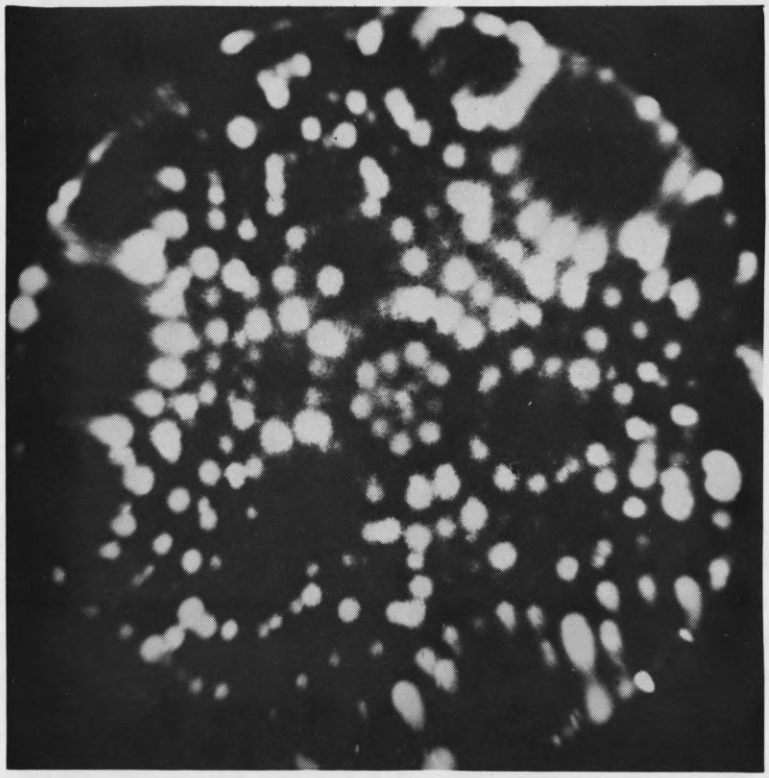

(d)

Fig 9. Steps in locating position of adatom on (111) plane.
c. (111) plane trimmed by pulsed field evaporation to resolve individual atoms.
d. Superposition of (a) upon (c) to reveal adatom position relative to substrate.

3. Images of the first and fourth lattice layers must superpose exactly.

4.2 Results

By proceeding in this fashion we have been able to identify[16] two different binding sites for tungsten adatoms on the (111) plane. In a total of 175 sequences which satisfy the criteria just stated, we have found adatoms only on lattice sites and on fault sites. No other positions have ever been observed. In 165 of the sequences, tungsten adatoms were located at lattice sites (Fig. 10b); in the remaining 10, on fault sites (Fig. 10c). In all these sequences the surface was brought to $\sim 300^{\circ}$ K for 60 sec, in the absence of an applied field, after deposition and imaging of the adatom. The location of the adatom was then again recorded photographically. This was done in an attempt to equilibrate the adatom with the lattice, to try to reduce the effects of the kinetics of the deposition event upon the location of the adatom on the surface. In no instance was any motion of the adatom observed during this heating cycle, indicating that the atoms were trapped in fairly deep potential wells.

The stability of adatoms at lattice and fault sites was further explored in a limited number of experiments, by bringing the (111) to considerably higher temperatures. With the adatom at a lattice site, heating the surface to 550° K produces no change in the position observed. The behavior of adatoms observed at a fault site

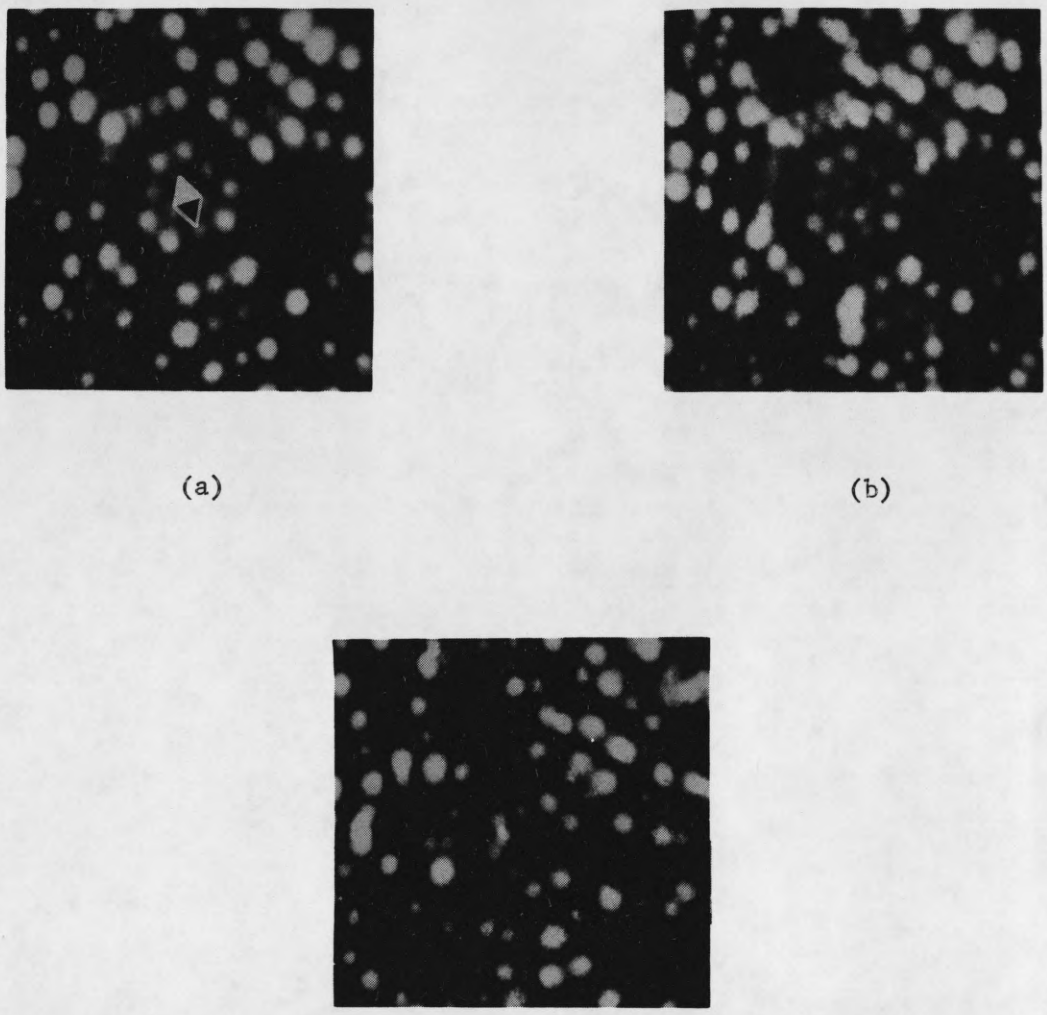

(a) (b)

(c)

Fig. 10. Adatom positions on (111) plane of tungsten.
a. Unit cell on the (111); solid triangle indicates location of atom 2 in Fig. 4.
b. Tungsten adatom on lattice site.
c. Tungsten adatom on fault site.

after deposition on a cold emitter is different. Heating to 480° K has been found to move the adatom out of the fault site and into an adjoining lattice postion. Three conclusions follow:

1. In our primary observations of the location of tungsten adatoms on the (111), the frequency with which lattice and fault sites are occupied is not dictated by the thermodynamics of binding, but by other, presumably kinetic, considerations.

2. The barrier preventing atom transfer from a fault to a lattice site is high, on the order of an electron volt.

3. Tungsten atoms are more firmly bound at lattice sites than they are at fault sites.

We envision the filling of the two types of sites as follows. An atom from the vapor source at $\approx 2500^{\circ}$ K strikes the surface. It is generally agreed that on first impact enough energy is exchanged with the lattice[17] to prevent re-emission from the surface. However, the atom may still be highly excited vibrationally; while in this state, it should be able to move from one site to another, losing additional energy at each. Experiments[18] suggest that the number of sites visited during this energy equilibration is small, certainly less than 100, but there is no information available specifically for the (111). Regardless of these details, however, if a vibrationally excited atom jumps into a fault site after having already undergone several collisions with the lattice, it may lose just enough energy to be trapped there permanently. Atoms at a fault site are in a shallower

potential well than at a lattice site. During equilibration with the lattice they will therefore be able to escape more readily than atoms at a lattice site. This will help to establish the preponderance of atoms actually observed at lattice sites. There may, of course, be differences in the exchange dynamics at the two sites as well. In any event, our observations identify only two sites on the (111) plane at which tungsten atoms are bound: above atom 2, at a fault site, and above atom 3, at a lattice site. Of the two, the latter is favored, both during the initial deposition and in high temperature equilibration.

5. FIELD EFFECTS

Up to this point we have ignored one very important question: does the act of observation affect the location of tungsten adatoms on the (111)? The conditions necessary for imaging in the field ion microscope are quite severe. Adatoms field evaporate from the (111) at 4.9 V/Å; for emitters with a radius of 150-200 Å, typical of our experiments, helium images of the (111) plane are best at a field of 4.5 V/Å.[19] Although this is a safe margin to avoid loss of atoms by evaporation, how can we be sure that the position of atoms revealed in the field ion microscope is also representative of their location in an ordinary thermal environment, in the absence of high fields? That this is indeed the case has been established in several different ways.

5.1 Observations at Low Fields

The act of imaging can affect adatoms through several mechanisms. In an applied field F, the potential energy of a neutral atom of polarizability α_A is lowered by $\frac{1}{2}\alpha_A F^2$. In actual fact an atom chemisorbed at a surface is in general not neutral; even in the absence of a field, atoms at a surface are polarized, and are characterized by a dipole moment μ. If we denote the total field energy of an atom by P(F), then[20]

$$P(F) = \mu F + \frac{1}{2}\alpha_A F^2 \quad . \tag{1}$$

At the low temperatures at which imaging is done, equilibrium will be dictated primarily by the internal energy of the system. If the potential energy of the atom at the surface in the absence of a field is denoted by $V(\underset{\sim}{R}_m)$, then at equilibrium in a field adatoms will seek to occupy sites at which $V(\underset{\sim}{R}_m)-P(F)$ is minimized; that is, in a field there will be a force acting on adatoms, tending to drive them toward positions $\underset{\sim}{R}_m$ at which the polarization term $|P(F)|$ is maximized. This will of course be balanced by changes in the binding energy as the location $\underset{\sim}{R}_m$ of the atom is changed.

Above and beyond this, the presence of the image gas also exerts an effect. The gas atoms are accelerated[10] by the inhomogeneous electric field around the tip, gaining an energy $\frac{1}{2}\alpha_g F^2$ before colliding with the surface. During imaging, the surface is covered with a layer of the imaging gas[21] and is in addition subjected to electron showers[22-25] from gas atoms that ionize in space beyond the critical distance, at

which the electron level of the atom is lined up with the Fermi energy of the metal. The importance of these events is difficult to evaluate. However, electron showers play only a small role in field evaporation of metal atoms. Even if a metal adatom were to be ionized by electron impact, electron exchange with the surface should result in rapid neutralization. This expectation is confirmed by the small cross-section for electron stimulated desorption found for metallic layers.[26]

Collisions with energetic gas atoms are more serious, but the kinetic energy of the image gas is still small. At the best image field it amounts to 0.15 eV for helium, and 0.17 eV for neon. On clean tungsten, energy exchange with the image gas is poor, the accommodation coefficient[27] for helium and neon amounting to less than 0.1. Of course during photography the image gas adsorbed at the surface will promote accommodation to some extent. However, the total energy imparted to the surface in any collision is minor by comparison with the effects of surface polarization. This is also the conclusion drawn from experiments on field evaporation. There it has been found that in helium, evaporation occurs at fields only 2% less than in a vacuum.[28]

Direct field effects, as given by Eq. (1), appear to be most important. The polarizability of tungsten atoms, deduced from experiments on field evaporation, is 4.80 Å^3 at kink sites, and 5.24 Å^3 on the (110) plane.[29,30] Assuming an average value of 5 Å^3 for α_A, the polarization energy amounts to 3.5 eV at the best image field for

helium, and 2.2 eV for neon, overshadowing in magnitude the energy exchange in collisions with the image gas. Field-dipole interactions are less significant. The dipole moment of W adatoms on the (110) has been estimated[31] at $\sim$ 1 D; on a rough plane like the (111) we expect a much smaller value. However, even with a moment of this size the first term in Eq. (1) only amounts to .9 eV when imaging with He,and .7 eV with Ne. We shall therefore neglect field-dipole interactions, and concentrate entirely on polarization effects.

To assess the importance of field and imaging effects upon the location of atoms at the surface, we have made observations of atomic positions at reduced fields. Using neon, the best image field[10] amounts to 80% of that for helium, and usable images of adatoms were obtained at 3.7 V/Å. In all studies with neon only the lattice and the fault sites have been found occupied by adatoms, with the former again predominant. Observations at even lower fields are possible with helium. Reasonable images of the (111) and of adatoms are obtained at 60% of the best image field, that is, at 2.8 V/Å. At no time was any motion of an adatom observed as the field was brought to the normal image strength; adatoms were found only at lattice and fault sites, in the usual ratio.

5.2 Surface Diffusion in High Fields

It can still be argued that the position of the atom may be seriously affected even at these reduced fields. Under the mildest conditions used for imaging, polarization reduces the energy of a

tungsten adatom by 1.3 eV. In absolute terms this is a substantial effect. The energy[32] to remove a tungsten atom from a kink site into the vapor amounts to 8.83 eV. However, what really counts in our work are differences in field effects at different sites, which will tend to shift the atom from one position to another. These can be ascertained directly by measuring the effect of the field upon atomic diffusion.

The diffusion coefficient for adatoms at a surface will be represented as usual[33] by

$$D = D_o \exp - \frac{V_D}{kT} \quad , \tag{2}$$

where V_D represents the height of the barrier restricting surface migration. The pre-factor D_o in two-dimensional diffusion is related to the jump length ℓ as well as to the attempt frequency ν through

$$D_o = \frac{\nu \ell^2}{4} \exp \frac{\Delta S}{k} \; ; \tag{3}$$

here ΔS is just the entropy of activation. In all experiments on the migration of single atoms it has been found that $\Delta S \approx 0$, and that the pre-factor can be adequately approximated by $D_o \approx 10^{-3}$ cm^2/sec. We shall throughout adopt this value. Surface diffusion in an applied field will be affected primarily through changes in the barrier to diffusion V_D, and we shall concentrate entirely upon this effect. The barrier is to a good approximation given by the difference in the potential energy of an adatom at a saddle position and at an equilibrium binding site on the surface. The increase in the barrier due to

the applied field, $\Delta V_D(F)$, is just a reflection of the difference in the field energy of an atom at the two sites. If we denote the saddle position by the subscript s and the equilibrium site by e, then

$$\Delta V_D(F) = -\frac{1}{2}\left[\alpha_s F_s^2 - \alpha_e F_e^2\right] . \tag{4}$$

To a first approximation the effective field at the saddle point, F_s, and at the equilibrium binding site, F_e, stand in a constant ratio to the applied field F. By introducing an effective polarizability α, we can express the polarization terms, again neglecting field-dipole effects, as[34]

$$\Delta V_D(F) = -\frac{1}{2}\alpha F^2 \tag{5}$$

where

$$\alpha \equiv \left[\alpha_s c_s - \alpha_e c_e\right] \tag{5a}$$

and

$$F_s \equiv c_s F \ , \ F_e \equiv c_e F \ . \tag{5b}$$

The diffusion coefficient in the presence of a uniform field now becomes

$$D = D_o \exp - \frac{\left[V_D - \frac{1}{2}\alpha F^2\right]}{kT} . \tag{6}$$

A determination of the change in the barrier to diffusion while imaging will therefore provide an indication of the driving force for displacement of an adatom under these conditions. Detailed diffusion studies on the (111) are extremely difficult, as in the absence of fields tungsten adatoms only begin to move over the surface at high temperatures, at which contamination by diffusion of impurities up the

shank also sets in. Instead, we have estimated changes in the barrier to diffusion by measuring the effect of the applied field (always in the presence of the image gas) upon the onset of diffusion. This is established as follows.

A tungsten atom is deposited at or near the center of a (111) plane. The tip voltage is then set at a fixed value and the temperature of the sample is raised, a little at a time, under continuous observation, until the atom is seen to move. Once the atom shifts its position in the field, it always moves by the shortest path across the edge of the (111) plane. This, of course, is the expected behavior. There is a field gradient across a flat surface on an emitter, with the field increasing from the center toward the edges. Once an atom jumps out of the center region, it finds itself in a higher field, and is there confronted by a lower barrier to diffusion. The limiting step in moving the atom off the plane is the crossing of the first potential barrier.

In the absence of an applied field, diffusion of adatoms becomes noticeable at temperatures $T \approx 600^{o}$ K. Because of problems with contamination, only a few observations have been done under unequivocal conditions. However, when a tungsten adatom at a layer site moves it is always found to jump to a layer site adjacent to it. Such a sequence is shown in Fig. 11.

The effect of the applied field upon the temperature at which diffusion first occurs is plotted in Fig. 12. Initially

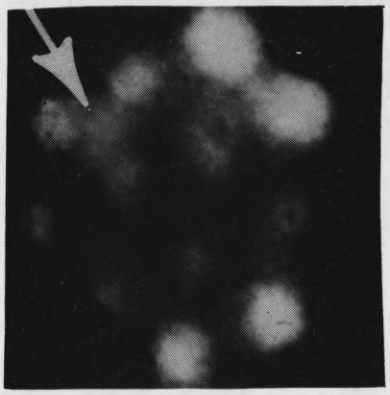

(a)

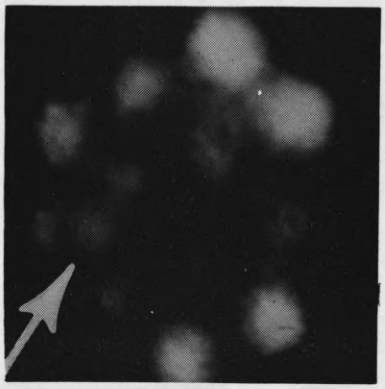

(b)

Fig. 11. Enlarged view of (111) plane, showing adatom displacement on warming.
a. Tungsten adatom, indicated by arrow, at a layer site.
b. Same plane, after heating to 600° K. Adatom has moved to adjacent layer site.

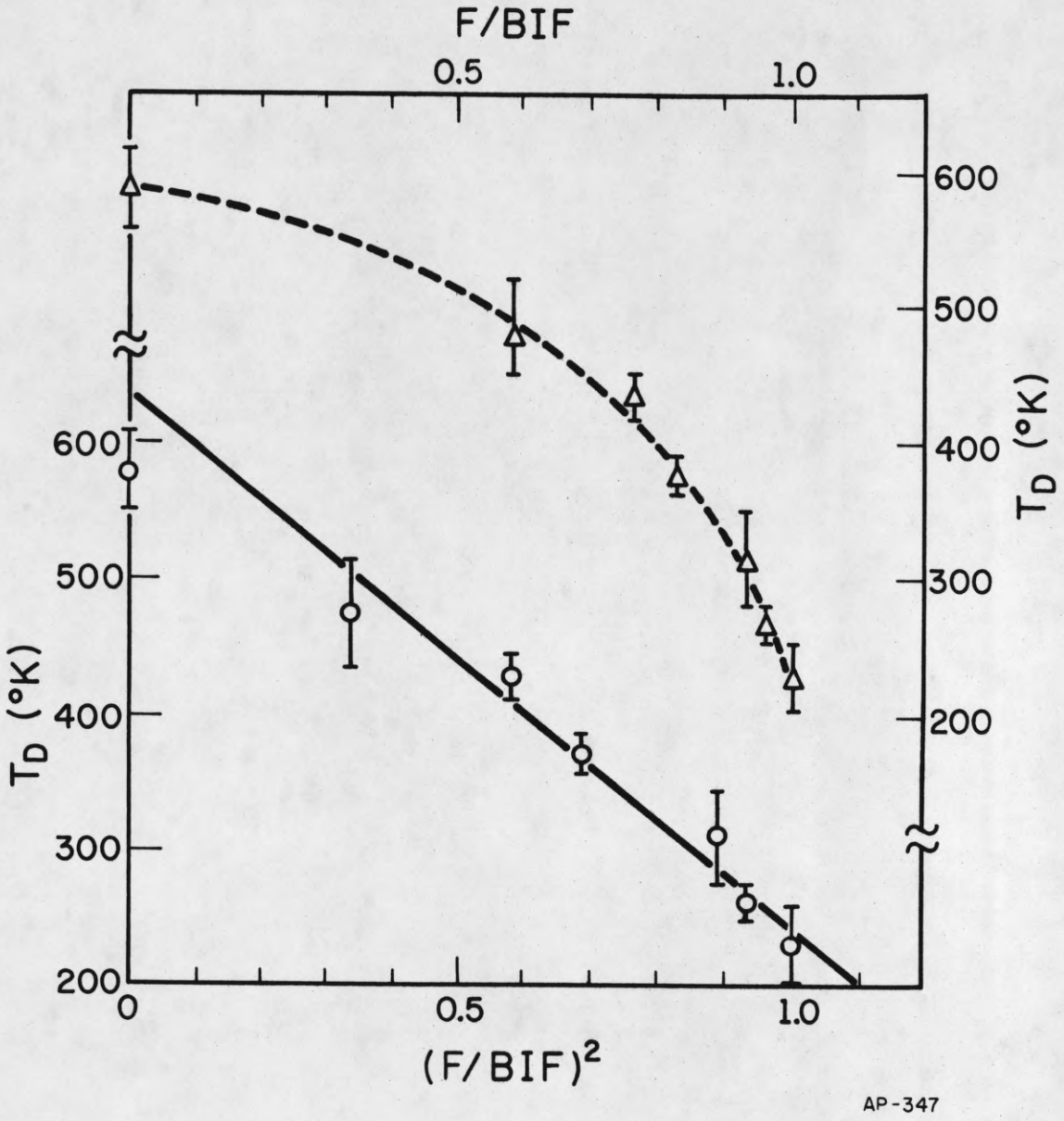

Fig. 12. Temperature T_D for the onset of adatom diffusion on (111), as a function of applied field F. Dashed curve: T_D vs. field; solid curve: T_D vs. $(\text{field})^2$. Best image field (BIF) for (111) = 4.5 V/Å.

diffusion is but little affected. Only for fields of $\approx$ 3.5 V/Å and greater, that is above $\approx$ 75% of the best image field for helium, does the onset temperature drop rapidly. At the lowest fields at which a reasonable helium ion image can first be achieved, at 2.8 V/Å, the temperature for the onset of diffusion is still quite high, 500° K.

For such diffusion, we assume that the adatom is initially at the center of the plane, where the lateral field gradient is zero. The temperature at which diffusion is first noted, that is at which $D \approx 10^{-17}$ cm^2/sec, then gives us a measure of the effective barrier to diffusion, $V_D - \frac{1}{2}\alpha F^2$, through

$$V_D - \frac{1}{2}\alpha F^2 = kT_D \ln (D_o/D) \quad . \tag{7}$$

We can rewrite this in an entirely equivalent way as

$$T_D = \left(V_D - \frac{1}{2}\alpha F^2\right)/C \tag{8}$$

$$C \equiv k \ln \left(D_o/D\right) ,$$

to emphasize that the temperature at which diffusion is first observed should vary linearly with F^2. A plot of this type has two advantages. It makes extrapolation to field free diffusion simple, and it also allows us to arrive at a value of the effective polarizability α. The former is important. As already noted, diffusion on the (111) in the absence of an applied field occurs at temperatures at which the intrusion of contaminants becomes troublesome. A separate check on the diffusion temperature is therefore desirable.

Our observations on the effect of the applied field upon the onset of diffusion are in fact best represented by a plot of temperature against F^2, as is evident in Fig. 12. This supports the notion that polarization, rather than some other field related phenomenon, is dominant. The extrapolated value of the diffusion temperature T_D estimated in this way, $640 \pm 20^{\circ}$ K, agrees reasonably well with the value observed directly. It should be noted that the polarizability term derived from the slope, $\alpha = 1.5 \pm .1$ Å^3, is only one third the polarizability of an adatom found by field evaporation.[29,30] This is expected in view of the different significance of the terms in the two experiments.[35] From the defining relation (5a), the polarizability term α deduced from diffusion in a field should be smaller in magnitude than for evaporation, and that is indeed found.

Most important in our context is that with these data we can attempt to assess the effect of the applied field upon the diffusion barrier. For diffusion over the (111) in the absence of an applied field, we deduce from Eq. (6) a barrier height of 1.8 eV. Observations of adatoms have been successfully made at fields as low as 2.8 V/Å. Under these conditions the field has lowered the barrier to diffusion by only 22%; that is, the activation energy to diffusion is still 1.4 eV. This is the potential which an adatom faces at an equilibrium site, whatever that may be, and which separates it from the saddle position. When measured by this yardstick the effect of the applied field is small and, at the low temperature at which site observations

have been conducted, interchange between atoms at a normal site and at the saddle is impossible.

Furthermore, from the diagram of the (111) plane in Fig. 4, it is clear that the only sites in the vicinity of the lattice sites, at which our observations have located the preponderance of adatoms, are ridge positions. If, playing the devil's advocate, we were to postulate the ridge as the site preferred by adatoms in the absence of the field, we would be hard pressed to understand how the energy of this site could differ so little from that of a lattice site for the latter to be favored in the field. The field, after all, only seems to change the diffusion barrier by ≈ 0.4 eV. Also, as the field is raised, from the lowest values at which the adatoms can be studied to more normal conditions, we should expect further displacements if these are already significant at low values; polarization only becomes significant at high values of the field. However, such motions have never been observed.

5.3 Internal Checks

There are strong internal arguments against any displacement of adatoms in our experiments. If such displacements were to occur, then on repeated viewing a given adatom should occasionally appear on one side of the normal site and then on the other. In fact, no change in the location of an adatom has ever been found when observed repeatedly at low temperatures. The frequency of occupation of alternate sites should be greater at higher temperatures. Although detailed observations

are not available, there is no indication of this in the occasional measurements that we have made.

An entirely separate case can be made against the hypothesis that the fields necessary for imaging might dictate the occupation of the lattice site by an adatom. Although adatoms have most frequently been found at lattice sites, occasionally an adatom is located at a fault site also. Adatoms at fault sites are stable to imaging. They can be displaced on heating, however, and they then move to a lattice site. The observation of adatoms at fault sites by itself proves that the occupation of the lattice site is not dictated by the field.

There is an additional argument to suggest that field effects do not intrude in our identification of the binding sites on the (111). It is clear from the model of a (111) plane that at both of the sites at which adatoms have been located they sit in a hollow. We expect field effects to be less at such positions than at other sites, at which adatoms are more protruding. If polarization were to play a significant role in the location of atoms on the surface, it would tend to displace them out of, rather than into, the sites actually observed.

The evidence is thus overwhelming that the locations on the (111) plane identified in our experiments as binding sites are appropriate, not just to the high field conditions under which they are observed, but to an ordinary thermal environment as well.

6. ATOM BINDING ON THE (111)

By direct observation in the field ion microscope two locations have been identified on the (111) plane of tungsten as sites for self-adsorption of tungsten atoms: lattice positions and fault positions. At the former, an adatom is centered between three atoms in the first crystal layer and above another in the third. At a fault site the adatom is positioned above a lattice atom in the second layer. In our experiments the frequency of occupation of lattice sites is dictated by the kinetics of atom deposition at the surface, and adatoms predominate at lattice rather than at fault sites. Lattice sites are also favored thermodynamically. This emerges on observation of atom diffusion from one site to another. As is apparent from the diagram of the unit cell of the (111) plane, in Fig. 4, the two sites are next to each other, but separated by a ridge position. The activation energy for motion of an atom out of a fault site and into a layer site, estimated from the temperature at which this first occurs, is $\approx$ 1.3 eV. In contrast, motion between lattice sites, which from the symmetry of the surface should involve a fault site as an intermediary, occurs over a barrier of $\approx$ 1.8 eV. It is clear that the binding energy of a tungsten adatom at a lattice site exceeds that at a fault site by $\approx$ 0.5 eV.

Our observations are qualitatively in accord with expectations for a lattice in which the cohesive energy can be described in terms of pair-wise interactions. Rough estimates of atom binding on a rigid lattice have been made by Neustadter and Bacigalupi,[36] based on the use

of Lennard-Jones potentials to represent interatomic interactions. These suggest a potential minimum at a lattice site and a secondary minimum at a fault site. More realistic estimates, in which the lattice is allowed to relax around the adatom, have been made by Ayrault.[37] These calculations, using Morse potentials, again indicate that an adatom at a lattice position will have the lowest potential energy. However, Ayrault locates the energy of an adatom at the fault site 2.5 eV above the minimum at a lattice site. This is in marked contrast with our experiments, which suggest that adatoms are quite strongly held at fault sites. Although a reliable value of the binding energy of tungsten adatoms on the (111) plane of tungsten is not available, it is probably on the order of 6 eV.[32] On this scale of energies the difference in the potential of adatoms at lattice and fault sites is small, amounting to less than 10% of the total binding. It will be interesting to explore more fully the implications of the unexpected stability of adatoms at fault sites.

Most important, however, is the fact that we have for the first time a quantitative determination of where metal atoms sit on the surface of their own lattice. Extensions of such measurements to other metals is routine, and should allow a more detailed exploration of interatomic forces on crystals.

ACKNOWLEDGMENTS

This work owes much to the unstinting efforts of the glass-blowing, photographic, and machine shops of the Coordinated Science Laboratory; it is a pleasure to acknowledge their contributions.

REFERENCES

1. For surveys of the present status of low energy electron diffraction, see

   a. M. B. Webb and M. G. Lagally, Solid State Phys. 28 (1973) 302.

   b. C. B. Duke, N. O. Lipari, and G. E. Laramore, Nuovo Cimento, To be published.

2. R. L. Park, in The Structure and Chemistry of Solid Surfaces, edited by G. A. Somorjai (J. Wiley, New York, 1969), p. 28-1.

3. Scattering from domains is reviewed by P. J. Estrup and E. G. McRae, Surface Sci. 25 (1971) 1.

4. C. W. Tucker, Jr. and C. B. Duke, Surface Sci. 29 (1972) 237.

5. S. Andersson and J. B. Pendry, J. Phys. C. 5 (1972) 241.

6. F. Forstmann, W. Berndt, and P. Büttner, Phys. Rev. Lett. 30 (1973) 17.

7. J. E. Demuth, D. W. Jepsen, and P. M. Marcus, Phys. Rev. Lett. 31 (1973) 540.

8. S. Andersson, B. Kasemo, J. B. Pendry, and M. A. Van Hove, Phys. Rev. Lett. 31 (1973) 595.

9. C. B. Duke, N. O. Lipari and G. E. Laramore, J. Vac. Sci. Technol., To be published.

10. For a general review of the technique and its capabilities, see

   a. E. W. Müller and T. T. Tsong, Field Ion Microscopy (American Elsevier, New York, 1969).

   b. K. M. Bowkett and D. A. Smith, Field-Ion Microscopy (North-Holland, Amsterdam, 1970).

11. A. van Oostrom, Phillips Res. Rep. 25 (1970) 87.

12. D. A. Reed, M.S. Thesis, University of Illinois at Urbana-Champaign, 1974.

13. J. F. Nicholas, An Atlas of Models of Crystal Surfaces (Gordon and Breach, New York, 1965).

14. Attempts of this sort on [110] oriented tungsten have previously been reported by G. D. W. Smith as well as by D. N. Seidman, 18th Field Emission Symposium, Eindhoven, The Netherlands, August, 1971.

15. See, for example, G. Ehrlich, Adv. Catalysis, 14 (1963) 255.

16. A preliminary account of these findings has been given by W. R. Graham and G. Ehrlich, J. Chem. Phys. 59 (1973) 3417.

17. B. McCarroll and G. Ehrlich, in Condensation and Evaporation of Solids, edited by E. Rutner, D. Goldfinger and J. P. Hirth (Gordon and Breach, New York, 1964) p. 521.

18. G. Ehrlich, in Metal Surfaces: Structure, Energetics and Kinetics (ASM, Metals Park, Ohio, 1963) p. 221.

19. Estimates of the electric field are throughout based on a value of 6 V/Å for the field at which tungsten evaporates at 20° K.

20. R. Gomer and L. W. Swanson, J. Chem. Phys. 38 (1963) 1613.

21. E. W. Müller, S. B. McLane and J. A. Panitz, Surface Sci. 17 (1969) 450.

22. R. D. Young, Seventh Field Emission Symposium, Linfield Research Institute, McMinnville, Oregon, 1960.

23. G. Ehrlich and F. G. Hudda, Philos. Mag. 8 (1963) 1587.

24. D. W. Bassett, Brit. J. Appl. Phys. 18 (1967) 1753.

25. A. E. Bell, L. W. Swanson and D. Reed, Surface Sci. 17 (1969) 418.

26. T. E. Madey and J. T. Yates, Jr., J. Vac. Sci. Technol. 8 (1971) 525.

27. L. B. Thomas, in Fundamentals of Gas-Surface Interactions, edited by H. Saltsburg, J. N. Smith, Jr., and M. Rogers (Academic, New York, 1967) p. 346,

28. O. Nishikawa and E. W. Müller, J. Appl. Phys. 35 (1964) 2806.

29. T. T. Tsong, J. Chem. Phys. 54 (1971) 4205.

30. M. Vesely and G. Ehrlich, Surface Sci. 34 (1973) 547.

31. K. Besocke and H. Wagner, Phys. Rev. B8 (1973) 4597.

32. G. Ehrlich and C. F. Kirk, J. Chem. Phys. 48 (1968) 1465.

33. See, for example, G. Ehrlich, in Proceedings of the International Summer Institute in Surface Science, Milwaukee 1973, In Press.

34. L. W. Swanson, R. W. Strayer and F. M. Charbonnier, Surface Sci. 2 (1964) 177.

35. T. T. Tsong and R. J. Walko, Phys. Status Solidi A 12 (1972) 111.

36. H. E. Neustadter and R. J. Bacigalupi, Surface Sci. 6 (1967) 246.

37. G. Ayrault, Ph.D. Thesis, University of Illinois at Urbana-Champagin, 1974.

Security Classification

DOCUMENT CONTROL DATA - R & D

(Security classification of title, body of abstract and indexing annotation must be entered when the overall report is classified)

1. ORIGINATING ACTIVITY *(Corporate author)*

Coordinated Science Laboratory
University of Illinois
Urbana, Illinois 61801

2a. REPORT SECURITY CLASSIFICATION

UNCLASSIFIED

2b. GROUP

3. REPORT TITLE

DIRECT IDENTIFICATION OF ATOMIC BINDING SITES ON A CRYSTAL

4. DESCRIPTIVE NOTES *(Type of report and inclusive dates)*

5. AUTHOR(S) *(First name, middle initial, last name)*

William R. Graham and Gert Ehrlich

6. REPORT DATE	7a. TOTAL NO. OF PAGES	7b. NO. OF REFS
July, 1974	49	37

8a. CONTRACT OR GRANT NO.	9a. ORIGINATOR'S REPORT NUMBER(S)
DAAB-07-72-C-0259	
b. PROJECT NO. AFOSR 72-2210	R-656
c.	9b. OTHER REPORT NO(S) *(Any other numbers that may be assigned this report)*
d.	UILU-ENG 74-2222

10. DISTRIBUTION STATEMENT

Approved for public release. Distribution unlimited.

11. SUPPLEMENTARY NOTES	12. SPONSORING MILITARY ACTIVITY
	Joint Services Electronics Program through U.S. Army Electronics Command and Air Force Office of Scientifitc Research

13. ABSTRACT

The atomic resolution of the field ion microscope, in conjunction with its ability to remove and identify individual atomic layers, has been used to map unambiguously the unit cell of the (111) plane of tungsten and to determine directly the location of single tungsten atoms adsorbed on this plane. Adatoms have been observed to occupy two binding sites only. The predominant site corresponds to a normal lattice position. The second site is of similar symmetry, in that the adatom sits between three first layer atoms; however, at this position the adatom is located above an atom in the second rather than the third lattice layer. The former site is favored energetically, but only by $\approx \frac{1}{2}$ eV. All observations have been made at high fields, but it is shown from studies of migration and other effects that the binding sites identified in the field ion microscope are typical of a normal, field free environment.

DD FORM 1 NOV 65 1473

Security Classification

14 KEY WORDS	LINK A		LINK B		LINK C	
	ROLE	WT	ROLE	WT	ROLE	WT
Atomic Binding Sites						
Adatom						